Journal of Neurochemistry

JOURNAL OF NEUROCHEMISTRY | 2015 | 133 | 750–765 doi: 10.1111/jnc.13039

ORIGINAL ARTICLE

Quantitative expression proteomics and phosphoproteomics profile of brain from PINK1 knockout mice: insights into mechanisms of familial Parkinson's disease

Judy C. Triplett,* Zhaoshu Zhang,* Rukhsana Sultana,* Jian Cai,† Jon B. Klein,† Hansruedi Büeler‡,§ and David Allan Butterfield*,¶

*Department of Chemistry, University of Kentucky, Lexington, Kentucky, USA
†Proteomics Center, University of Louisville, Louisville, Kentucky, USA
‡Department of Anatomy and Neurobiology, University of Kentucky, Lexington, Kentucky, USA
§Harbin Institute of Technology, School of Life Science and Technology, Harbin, China
¶Center of Membrane Sciences and Sanders-Brown Center on Aging, University of Kentucky, Lexington, Kentucky, USA

Abstract

Parkinson's disease (PD) is an age-related, neurodegenerative motor disorder characterized by progressive degeneration of dopaminergic neurons in the substantia nigra pars compacta and presence of α-synuclein-containing protein aggregates. Mutations in the mitochondrial Ser/Thr kinase PTEN-induced kinase 1 (*PINK1*) are associated with an autosomal recessive familial form of early-onset PD. Recent studies have suggested that PINK1 plays important neuroprotective roles against mitochondrial dysfunction by phosphorylating and recruiting Parkin, a cytosolic E3 ubiquitin ligase, to facilitate elimination of damaged mitochondria via autophagy-lysosomal pathways. Loss of PINK1 in cells and animals leads to various mitochondrial impairments and oxidative stress, culminating in dopaminergic neuronal death in humans. Using a 2-D polyacrylamide gel electrophoresis proteomics approach, the differences in expressed brain proteome and phosphoproteome between 6-month-old PINK1-deficient mice and wild-type mice were identified. The observed changes in the brain proteome and phosphoproteome of mice lacking PINK1 suggest that defects in signaling networks, energy metabolism, cellular proteostasis, and neuronal structure and plasticity are involved in the pathogenesis of familial PD.

Keywords: expression proteomics, knockout mouse, Parkinson's disease, phosphoproteomics, PINK1.
J. Neurochem. (2015) **133**, 750–765.

This article is related to a companion paper: doi: 10.1111/jnc.13037.

Parkinson's disease (PD) is the most common neurodegenerative movement disorder. The relative risk of developing PD increases with age and approximately 1–2% of the population above 65 years is affected (Twelves *et al.* 2003; Pilsl and Winklhofer 2012). PD is characterized by the accumulation of Serine-129 phosphorylated α-synuclein aggregates (Anderson *et al.* 2006) within Lewy bodies and the loss of the majority of dopaminergic (DA) neurons in the substantia nigra pars compacta, causing drastically diminished dopamine release in the striatum (Braak *et al.* 2003). In addition to the cardinal motor symptoms (resting tremor, bradykinesia, rigidity, postural instability), PD patients frequently suffer from a variety of non-motor symptoms that may occur decades earlier and include cognitive decline, depression, hallucinations, REM sleep disorder, and anosmia (Chaudhuri *et al.* 2006; Jankovic 2008). Although the

Received October 21, 2014; revised manuscript received December 8, 2014; accepted January 12, 2015.

Address correspondence and reprint requests to Prof D. Allan Butterfield, Department of Chemistry, Center of Membrane Sciences, and Sanders-Brown Center on Aging, University of Kentucky, Lexington, KY 40506-0055, USA. E-mail: dabcns@uky.edu

Abbreviations used: APT1, acyl-protein thioesterase 1; DA, dopaminergic; KO, knockout; PARL, presenilins-associated rhomboid-like protein; PD, Parkinson's disease; PHB, prohibitin; PINK1, PTEN-induced kinase 1; PPIaseA, peptidyl-prolyl cis-trans isomerase A; PTEN, phosphatase and tensin homologue.

precise cause of PD remains elusive, significant contributing factors are believed to include exposure to environmental toxins, oxidative stress, inflammation, mitochondrial dysfunction, and failure of proteostasis networks associated with protein aggregation (Henchcliffe and Beal 2008; Bueler 2009; Tansey and Goldberg 2010).

While the majority of PD cases are sporadic, an estimated 5–10% of patients develop PD as a result of inheritable mutations in one of several genes (Gasser *et al.* 2011). Mutations in *Pink1* are the second most common cause of autosomal recessive familial early-onset PD (Valente *et al.* 2004; Bonifati *et al.* 2005; Bonifati 2012). PINK1 is a mitochondrial kinase consisting of 581 amino acids that encode for a mitochondrial targeting sequence, a transmembrane domain and a Ser/Thr kinase domain. PINK1 is believed to confer neuroprotection by policing mitochondrial integrity (Narendra *et al.* 2010; Jin and Youle 2012), and a growing amount of research links dysfunction of mitochondrial dynamics with PD (Heeman *et al.* 2011; Hauser and Hastings 2013; Van Laar and Berman 2013). DA neurons may be particularly vulnerable to mitochondrial dysfunction and oxidative stress because of reduced mitochondrial reserve compared to other types of neurons and the reliance on calcium influx for pace-making (Liang *et al.* 2007; Surmeier *et al.* 2011). In normal cells with healthy mitochondria, PINK1 is imported to the inner mitochondrial membrane where the N-terminal mitochondrial targeting sequence is cleaved by the mitochondrial protease, PARL (Deas *et al.* 2011; Meissner *et al.* 2011). Subsequently, PINK1 is retro-translocated to the cytosol where it is degraded by the proteasome (Yamano and Youle 2013). However, a proportion of PINK1 remains in the cytoplasm (Haque *et al.* 2008; Lin and Kang 2008) and cytosolic PINK1 has been implicated in the regulation of various pathways, including AKT signal transduction and cell survival, synaptic plasticity, DA synthesis, and mitophagy (Akundi *et al.* 2012; Fedorowicz *et al.* 2014; Haque *et al.* 2008; Murata *et al.* 2011; Zhou *et al.* 2014). Import of PINK1 to the inner mitochondrial membrane is blocked when the mitochondrial electron transport chain becomes dysfunctional and membrane potential ($\Delta\Psi_m$) is decreased (Matsuda *et al.* 2010; Amo *et al.* 2011). PINK1 then accumulates on the outer mitochondrial membrane where it phosphorylates Ser65 in the ubiquitin-like domain of the E3 ligase, Parkin, to initiate mitophagy (Kazlauskaite *et al.* 2014). When PINK1 kinase activity is inactivated in mice and flies via gene ablation, mitochondrial dysfunction ensues and structurally abnormal mitochondria accumulate in cells (Park *et al.* 2006; Exner *et al.* 2007; Gautier *et al.* 2008, 2012; Akundi *et al.* 2011, 2013; Heeman *et al.* 2011). Furthermore, mutations in *PINK1* cause a decrease in mitochondrial complex I activity and ATP production, as well as elevated production of reactive oxygen species (Deas *et al.* 2011; Koh and Chung 2012; Morais *et al.* 2014; Yuan *et al.* 2010).

In this study, we utilized a 2-D polyacrylamide gel electrophoresis (PAGE) proteomics approach to identify proteins with differential expression levels and phosphorylation states in the brains of PINK1 knockout (KO) mice versus wild-type controls to further study the molecular mechanisms of PINK1-related PD.

Materials and methods

Materials

All chemicals used in these studies were purchased from Sigma-Aldrich (St. Louis, MO, USA) with noted exceptions: Criterion precast polyacrylamide gels, ReadyStrip IPG strips, TGS and XT MOPS electrophoresis running buffers, 0.2 nm nitrocellulose membrane, Precision Plus Protein All Blue Standards, Sypro Ruby Protein Stain, mineral oil, dithiothreitol (DTT), iodoacetamide (IA), biolytes, and urea were purchased from Bio-Rad (Hercules, CA, USA). Pro-Q Diamond phosphoprotein stain, PeppermintStick phosphoprotein molecular weight marker, and anti-phosphoserine, anti-phosphothreonine, and anti-phosphotyrosine antibodies raised in rabbits were purchased from Invitrogen (Grand Island, NY, USA). Anti-HSP70 and anti-aldolase A (ALDOA) antibodies raised in rabbits were purchased from Cell Signaling Technology (Danvers, MA, USA). Anti-MAPK1/2 polycolonal antibody raised in rabbits, C_{18} ZipTips, and Re-Blot Plus Strong stripping solution were purchased from Millipore (Billerica, MA, USA). Calmodulin (CaM) polyclonal antibody raised in rabbits was purchased from Santa Cruz Biotechnology (Dallas, TX, USA). Amersham enhanced chemiluminescence (ECL) rabbit IgG horseradish peroxidase (HRP)-linked secondary antibody, protein A/G beads, and ECL-Plus western blotting detection reagents were purchased from GE Healthcare (Pittsburgh, PA, USA). Modified trypsin solution was obtained from Promega (Madison, WI, USA). Pierce bicinchoninic acid Protein Assay Reagents A & B were purchased from Thermo Scientific (Waltham, MA, USA).

Animals and brain tissue

The male mice used in this study were provided by our collaborator and coauthor, Dr Hansruedi Büeler, when he was at the University of Kentucky. The generation and characterization of these PINK1-deficient mice has been described previously (Akundi *et al.* 2011). The animal housing facility regularly underwent serological testing to certify a healthy, virus, and pathogen free facility. Subjects were fed Richland Laboratory Rodent Diet 5001 and water *ad libitum*. The animal rooms were maintained with a 12 h light:12 h dark cycle (where lights were turned on at 6:00 a.m.) at 20–22°C. For the experimental groups of animals, $n = 6$ per group, whole brains were isolated from mice rendered unconscious by CO_2 inhalation and killed by cervical dislocation using procedures approved by the UK Institutional Animal Care and Use Committee. Dissected brains were flash-frozen in liquid nitrogen and stored at −80°C until use.

Sample preparation

Mouse brains were thawed and individual homogenates were prepared using a Wheaton glass homogenizer (~ 40 passes) with ice-cold isolation buffer (0.32 M sucrose, 2 mM EDTA, 2 mM

EGTA, 20 mM HEPES, 0.2 μg/mL phenylmethylsulfonyl fluoride, 4 μg/mL leupeptin, 4 μg/mL pepstatin, 5 μg/mL aprotinin, and 5 μg/mL phosphatase inhibitor cocktail 2). Homogenates were vortexed on ice and then sonicated on ice for 10 s at 20% power, two times, with a Fisher 550 Sonic Dismembrator (Pittsburgh, PA, USA). Protein concentrations of the homogenates were determined by the Pierce bicinchoninic acid method (Smith *et al.* 1985).

Two-dimensional polyacrylamide gel electrophoresis

Isoelectric focusing

Isoelectric focusing was performed as described previously (Sultana *et al.* 2007). Briefly, brain homogenate proteins (200 μg) were shaken for 2 h at 22°C in 200 μL of rehydration buffer [8 M urea, 2.0% (w/v) CHAPS, 2 M thiourea, 50 mM DTT, 0.2% Biolytes, 0.01% Bromophenol Blue]. Samples (200 μL) were applied to 11 cm pH 3–10 ReadyStrip IPG strips (linear gradient). Strips were actively rehydrated at 20°C for 18 h at 50 V. Next, the samples were isoelectrically focused at a constant temperature of 20°C beginning at 300 V for 2 h, 500 V for 2 h, 1000 V for 2 h, 8000 V for 8 h, and finishing at 8000 V for 10 h. IPG strips were stored at −80°C until second dimension separation (sodium dodecyl sulfate, SDS–PAGE).

SDS–PAGE

Isoelectric focusing strips were thawed and equilibrated with buffer A and buffer B (buffer A [50 mM Tris–HCl, pH 6.8, 6 M urea, 1% (w/v) SDS, 30% v/v glycerol, 0.5% DTT], buffer B [50 mM Tris–HCl, pH 6.8, 6 M urea, 1% (w/v) SDS, 30% v/v glycerol, 4.5% IA]). IPG strips were next placed into Criterion precast linear gradient (8–16%) Tris–HCl polyacrylamide gels, 1 IPG + 1 Well Comb, 11 cm. Invitrogen PeppermintStick molecular weight marker and samples were run at a constant voltage of 200 V for approximately 65 min in Tris-Glycine SDS running buffer.

Gel staining

Proteins and phosphoproteins were detected using SYPRO Ruby and Pro-Q Diamond phosphoprotein gel stain according to manufacturer's directions and as previously described (Di Domenico *et al.* 2011). Briefly, gels were fixed in solution [10% (v/v) acetic acid, 50% (v/v) methanol] (50 mL) and washed in deionized water. Next, 60 mL of Pro-Q Diamond stain was added with gentle rocking for 90 min. Gels were then destained four times for 30 min each in 100 mL of destaining solution [20% acetonitrile (ACN), 50 mM sodium acetate, pH 4]. The gels were washed in deionized water and scanned at 580 nm using a GE Healthcare Life Sciences Typhoon FLA 9500 scanner. The gels were then stained overnight with 50 mL of Sypro Ruby gel stain. Gels were rinsed and placed in deionized water. Gels were scanned at 450 nm and then stored at 4°C until protein spot excision.

Image analysis

Expression proteomics

Spot intensities from SYPRO Ruby-stained 2D-gel images of wild-type (WT) and PINK1 KO samples were quantified by densitometry using PDQuest 2-D Analysis Software (Bio-Rad). Intensities of each gel were normalized to the total density of each gel. Protein spots were manually and automatically matched with the PDQuest program. Spot densities in KO and WT samples were compared and spots with a statistically significant difference based on a Student's two-tailed *t*-test ($p < 0.05$) were considered for in-gel trypsin digestion and subsequent identification.

Phosphoproteomics

Protein spots from Pro-Q Diamond-stained 2D-gel images of *PINK1*$^{-/-}$ and WT samples were quantified and matched together in the same manner as the SYPRO Ruby-stained gels. Next, two master gels were chosen, one from the Pro-Q Diamond images and one from the Sypro Ruby-stained images. The phosphoprotein master image was then matched to the master Sypro Ruby-stained image in the same manner as described above. The PDQuest software provided numerical data corresponding to the intensity of the protein spot. The phosphoprotein spot densities were then normalized to the Sypro Ruby spot densities and the resultant normalized phosphoprotein spot densities in KO and WT samples were compared and spots with a statistically significant difference based on a Student's two-tailed *t*-test ($p < 0.05$) were considered for in-gel trypsin digestion and subsequent identification.

In-gel trypsin digestion/peptide extraction

Protein spots were excised from 2D-gels with a clean, sterilized razor blade and individually transferred to Eppendorf microcentrifuge tubes for trypsin digestion as previously described (Thongboonkerd *et al.* 2002). Gel plugs were incubated with 20 μL of 0.1 M ammonium bicarbonate (NH_4HCO_3) for 15 min, and with 30 μL of ACN for 15 min. Gel plugs were dried under a flow hood at 22°C for 30 min. Next, 30 μL of 20 mM DTT in 0.1 M NH_4HCO_3 was added at 56°C for 45 min. The DTT/NH_4HCO_3 solution was then removed and replaced with 30 μL of 0.05 M IA in 0.1 M NH_4HCO_3 and incubated at 22°C for 15 min. Next, the IA solution was removed and plugs incubated for 15 min with 150 μL of 0.05 M NH_4HCO_3 at 22°C. Then, 200 μL ACN was added to this solution and incubated for 15 min at 22°C. Solvent was removed and gel plugs were allowed to dry for 30 min at 22°C under a flow hood. Plugs were rehydrated with modified trypsin solution in 0.05 M NH_4HCO_3 (enough to completely cover the gel plugs) and incubated with shaking overnight at 37°C. The next day, the salts and contaminants were removed from the tryptic peptide solutions using C_{18} ZipTips in accordance with manufacturer's directions. Samples were stored at −80°C until MS/MS analysis.

NanoLC–MS with data-dependent scan

Samples desalted with C_{18} Zip Tips were reconstituted in 10 μL 5% ACN/0.1% formic acid (FA) and analyzed by a nanoAcquity (Waters, Milford, MA, USA)-LTQ Orbitrap XL (Thermo Scientific, San Jose, CA, USA) system in data-dependent scan mode. An in-house packed capillary column (0.1 × 130 mm column packed with 3.6 μm, 200Å XB-C18) and a gradient with 0.1% FA and ACN/0.1% FA at 200 nL/min were used for separation. The MS spectra were acquired by the orbitrap at 30 000 resolution and MS/MS spectra of the six most intense ions in MS scan were obtained by the orbitrap at 7500 resolution. Data files from each sample were searched against the most current version of the Swiss-Prot database by SEQUEST (Proteome Discoverer v1.4; Thermo Scientific). At

least two high-confidence peptide matches were required for protein identification (false discovery rate < 1%). Proteins matched with the same peptides are reported as one protein group.

Immunoprecipitation and western blotting validations

Immunoprecipitation

Whole brain homogenized protein extracts (250 μg) were suspended in 500 μL immunoprecipitation (IP) buffer [0.05% NP-40, leupeptin 4 μg/mL, pepstatin 4 μg/mL, aproprotin 5 μg/mL, phosphatase inhibitor cocktail 10 μg/mL in a phosphate buffer solution, pH 8 (8 M NaCl, 0.2 M KCl, 1.44 M Na_2HPO_4, 0.24 M KH_2PO_4, pH adjusted with NaOH)] and allowed to shake for 30 min at 4°C. Next, 50 μL of Protein A/G beads (per sample) was washed and centrifuged at 800 *g* for 5 min at 4°C. The washed beads were added to the individual protein samples to pre-clear of non-specific protein A/G artifacts for 90 min at 4°C. Samples were then centrifuged at 800 *g* for 5 min at 4°C and the supernatant was transferred to new Eppendorf tubes with either anti-MAPK1 antibody (1 : 50 dilution) or anti-CaM antibody (1 : 50) and shaken overnight at 4°C. The next morning, 50 μL of protein A/G beads was washed as and incubated with the protein samples for 90 min at 4°C. After removing the supernatant, the beads were again washed five times with IP buffer with 10 min of shaking in IP buffer between centrifugations. The beads were preserved for a 1D-PAGE experiment.

One-dimensional polyacrylamide gel electrophoresis

Whole brain homogenates (50 μg) or beads from IP experiments were suspended in 4X sample loading buffer [0.5 M Tris, pH 6.8, 40% glycerol, 8% SDS, 20% β-mercaptoethanol, 0.01% Bromophenol Blue] diluted to 1X with distilled water, heated at 95°C for 5 min and cooled on ice. Samples and Precision Plus Protein All Blue Standards were loaded into a Criterion precast (4–12%) Bis-Tris polyacrylamide 12 or 18 well gels and run at 22°C in XT MOPS running buffer at 80 V for 15 min. The voltage was then increased to 120 V for approximately 100 min at 22°C for the duration of the electrophoretic run.

1D-western blotting

1D-gels were directly transferred to nitrocellulose membranes (0.2 nm) using a Trans-Blot Turbo Blotting System (Bio-Rad). After the transfer, membranes were incubated in a blocking solution of 3% bovine serum albumin in Wash Blot [150 mM NaCl, 3 mM NaH_2PO_4, 17 mM $NaHPO_4$ and 0.04% (v/v) Tween 20] at 22°C for 1.5 h. Each protein of interest was detected by incubation with a primary antibody (1 : 8000 dilution), in blocking solution at 22°C with gentle rocking for 2 h. Blots were rinsed two times for 5 min each and one time for 10 min in Wash Blot, followed by a 1 h incubation with a HRP (1 : 3000) secondary antibody at 22°C with gentle rocking. Blots were rinsed three times for 5, 10, and 10 min each in Wash Blot and developed chemiluminescently using Clarity Western ECL substrate. After developing for 5 min at 22°C in the dark, blots were scanned using a Bio-Rad ChemiDoc XRS+ imaging system and quantified using Image Lab software (Hercules, CA, USA). Blots were rinsed and then stripped with Re-Blot Plus Strong solution for exactly 10 min at 22°C, followed by three 5 min rinses with Wash Blot. The membranes were then blocked once again in 3% bovine serum albumin for 1.5 h. Next, an anti-tubulin antibody (1 : 20 000) or anti-phosphoserine, anti-phosphothreonine and anti-phosphotyrosine antibodies (1 : 10 000) were added to the Wash Blot solution with 2 h more of gentle rocking at 22°C. Membranes were then washed, incubated with a secondary HRP-conjugated antibody, washed, developed chemiluminescently and scanned.

Statistical analysis

All statistical analyses were performed using a two-tailed Student's *t*-test, in which $p < 0.05$ was considered statistically significant for western blot and PDQuest analysis. Fold-change values of easily discernible protein spots were determined by dividing the average, normalized spot intensities in the knockout gels by the average, normalized spot intensities of the wild-type gels. Only spots with a 1.25-fold change or greater in normalized spot density were considered for MS/MS analysis. Protein and peptide identifications obtained with the SEQUEST search algorithm with $p < 0.01$ were considered to be statistically significant.

Results

Proteomic analyses of the isolated brain proteins were conducted using a 2D-PAGE approach with Sypro Ruby and Pro-Q Diamond staining in conjunction with MS/MS analysis. Protein spot intensities were compared between *PINK1*$^{(-/-)}$ and *PINK1*$^{(+/+)}$ control mice to determine differentially expressed and phosphorylated proteins. Figure 1 shows representative examples obtained from SYPRO Ruby-stained 2-D gel images of the isolated proteins from 6-month-old *PINK1*$^{(-/-)}$ and *PINK1*$^{(+/+)}$ mice with significant differentially expressed proteins labeled. Figure 2 shows typical images of Pro-Q Diamond-stained gels with protein spots showing altered phosphorylation states labeled in the images. Graphs displaying normalized phosphorylation intensity of each sample are also provided. PDQuest analysis of all of the 2-D images found 29 protein spots suitable for extraction and whose expression or phosphorylation state was significantly altered in the brains of *PINK1*$^{(-/-)}$ mice as compared to the WT controls. After in-gel trypsin digestion and peptide extraction, MS/MS analysis coupled to interrogation of protein databases was utilized to determine the identity of the proteins. Tables 1 and 2 list the proteins in the brains of *PINK1*$^{(-/-)}$ mice that showed significantly altered expression or phosphorylation states. Other information listed in the tables include: the spot number as labeled by the PDQuest program, the SwissProt accession number, percentage of the protein sequence covered by matching peptides, the number of peptide sequences identified by the MS/MS analysis, the protein confidence score, the expected molecular weight and isoelectric point of the identified protein, as well as the fold-change levels and *p*-values obtained from the PDQuest analysis. Regarding fold-change values, a ↑1.33-fold means

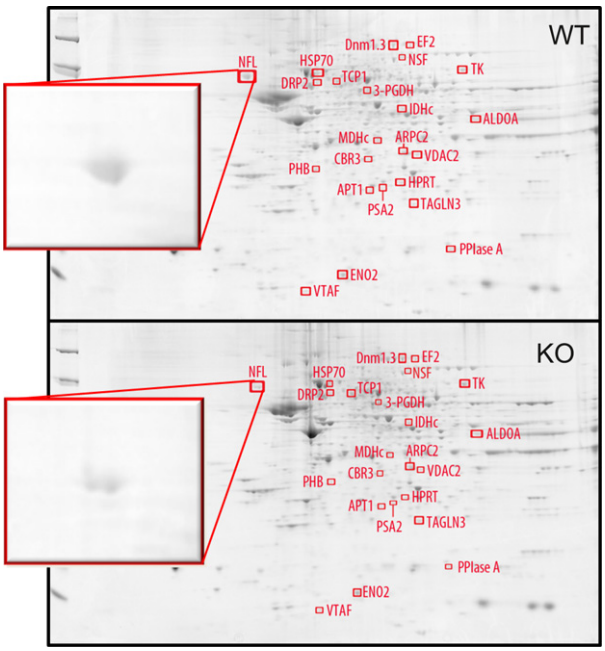

Fig. 1 Representative 2-D gel images of isolated proteins from the brains of 6-month-old wild-type (WT) mice and PINK1 knockout (KO) mice ($n = 6$). Proteins whose expression was significantly altered are labeled in the images and NFL spot is enlarged to demonstrate differential levels ($p < 0.05$).

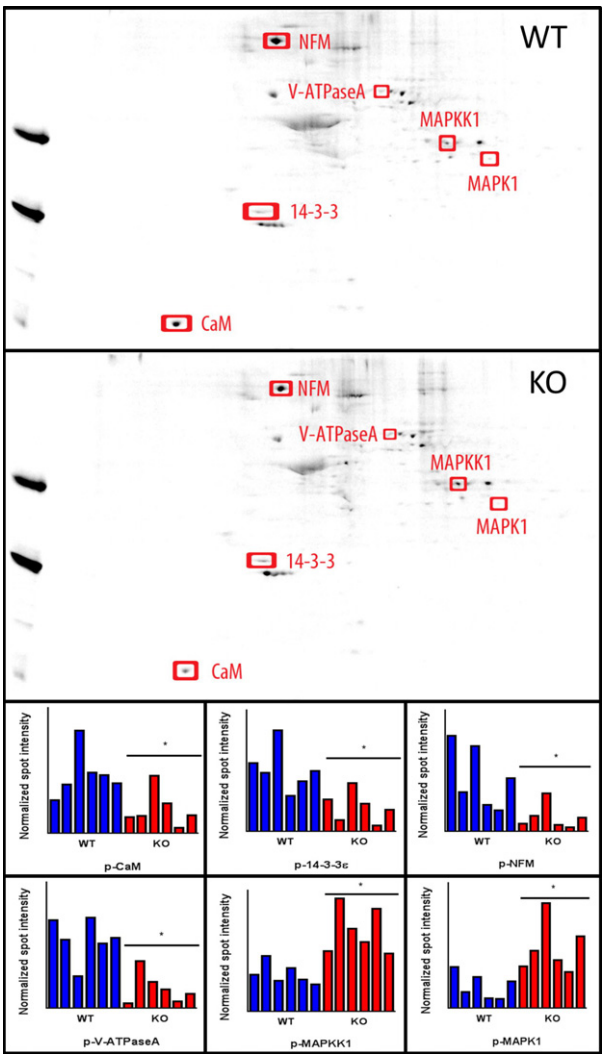

Fig. 2 Representative images of Pro-Q Diamond-stained 2-D gels with protein spots showing altered phosphorylation states labeled in the images. Bar graphs displaying normalized phosphorylation intensity (Pro-Q Diamond spot density divided by SYPRO Ruby spot density) of each of $n = 6$ wild-type (WT) (blue) and $n = 6$ knockout (KO) (red) samples [total of 12 individual gels] are also provided ($p < 0.05$).

the protein expression in the KO brain is 33% more than in WT brain. A ↓0.0885-fold means protein expression in the KO brain is 91.15% less than in WT brain. All proteins were identified by more than one peptide sequence. Furthermore, identified protein spots were visually compared against the theoretical molecular weights and isoelectric points from the mass spectrometry analysis. The 23 brain proteins with significantly altered expression were identified as: neurofilament light peptide (NFL) (↓0.580-fold), V-type proton ATPase subunit F (↓0.725-fold), prohibitin (PHB) (↓0.464-fold), dihydropyrimidinase-related protein 2 (DRP2, also called collapsing response-mediated protein 2, CRMP2) (↓0.0186-fold), heat-shock-related 70 kDa protein 2 (HSP70.2) (↓0.213-fold), acyl-protein thioesterase 1 (APT1) (↓0.0130-fold), carbonyl reductase [NADPH] 3 (CBR3) (↓0.0244-fold), proteasome subunit alpha type-2 (PSA2) (↓0.0898-fold), hypoxanthine-guanine phosphoribosyltransferase (HPRT) (↓0.0885-fold), malate dehydrogenase, cytoplasmic (↓0.0121-fold), actin-related protein 2/3 complex subunit 2 (ARPC2) (↓0.0110-fold), voltage-dependent anion-selective channel protein 2 (VDAC-2) (↓0.607-fold), isocitrate dehydrogenase [NADP] cytoplasmic (↓0.226-fold), vesicle-fusing ATPase (↓0.0396-fold), elongation factor 2 (EF2) (↓0.411-fold) and peptidyl-prolyl cis-trans isomerase A, also known as cyclophilin A (↓0.181-fold), gamma-enolase (ENO2) (↑1.24-fold), T-complex protein 1 subunit epsilon (↑1.33-fold), D-3-phosphoglycerate dehydrogenase (↑3.69-fold), isoform 3 of dynamin-1 (↑1.41-fold), transgelin-3 (↑1.47-fold), fructose-bisphosphate ALDOA (↑2.99-fold), and transketolase (↑1.52-fold). The six proteins found to have differential phosphorylation states were as follows: CaM (↓0.418-fold), 14-3-3 protein epsilon (↓0.480-fold), neurofilament medium polypeptide (NSF) (↓0.275-fold), V-type proton ATPase catalytic subunit A (↓0.313-fold), dual specificity mitogen-activated protein kinase kinase 1 (↑2.34-fold), and mitogen-activated protein kinase 1 (↑3.39-fold).

Table 1 PDQuest and MS/MS results of brain proteins with significantly altered expression in the PINK1 KO mice versus WT mice

Spot	Protein identified	Accession no.	Coverage (%)	Number of identified peptides	Score	MW (kDa)	pI*	*p*-value	Fold increase/ decrease
1701	Neurofilament light peptide (NFL)	P08551	31.12	13	104.31	61.5	4.64	0.012	0.580
2008	V-type proton ATPase subunit F (VTAF)	Q9D1K2	41.18	4	20.46	13.4	5.82	0.041	0.725
3202	Prohibitin (PHB)	P67778	44.12	10	53.45	29.8	5.76	0.0057	0.464
3603	Dihydropyrimidinase-related protein 2 (DRP2)	O08553	15.21	7	30.03	62.2	6.38	0.046	0.0186
3703	Heat-shock-related 70 kDa protein 2 (HSP70.2)	P17156	23.70	13	68.18	69.6	5.67	0.015	0.213
4111	Acyl-protein thioesterase 1 (fragment) (APT1)	J3QK48	14.55	3	9.37	23.2	6.77	0.0091	0.0130
4206	Carbonyl reductase [NADPH] 3 (CBR3)	Q8K354	26.35	7	43.45	30.9	6.57	0.048	0.0244
5102	Proteasome subunit alpha type-2 (PSA2)	P49722	14.96	2	6.67	25.9	7.43	0.0090	0.0898
5109	Hypoxanthine-guanine phosphoribosyltransferase (HPRT)	P00493	34.40	6	29.47	24.6	6.68	0.00011	0.0885
5303	Malate dehydrogenase, cytoplasmic (MDHc)	P14152	23.95	7	22.90	36.5	6.58	0.035	0.0121
6201	Actin-related protein 2/3 complex subunit 2 (ARPC2)	Q9CVB6	15.33	5	17.54	34.3	7.36	0.0092	0.0110
6210	Voltage-dependent anion-selective channel protein 2 (VDAC2)	G3UX26	12.37	3	10.04	30.4	7.58	0.043	0.607
6502	Isocitrate dehydrogenase [NADP] cytoplasmic (IDHc)	O88844	13.29	5	14.77	46.6	7.17	0.021	0.226
6701	Vesicle-fusing ATPase (NSF)	P46460	15.32	11	49.59	82.6	6.95	0.041	0.0396
6802	Elongation factor 2 (EF2)	P58252	3.38	3	19.70	95.3	6.83	0.042	0.411
7001	Peptidyl-prolyl cis-trans isomerase A (PPIaseA)	P17742	10.98	2	8.65	18.0	7.90	0.028	0.181
3007	Gamma-enolase (ENO2)	D3YVD3	25.41	2	3.81	13.4	5.15	0.014	1.24
3614	T-complex protein 1 subunit epsilon (TCP1)	P80316	17.19	9	50.59	59.6	6.02	0.012	1.33
4617	D-3-phosphoglycerate dehydrogenase (3-PGDH)	Q61753	12.76	6	38.81	56.5	6.54	0.0096	3.69
5814	Isoform 3 of dynamin-1 (Dnm1.3)	P39053-3	23.62	18	78.91	95.9	6.76	0.053	1.41
6104	Transgelin-3 (TAGLN3)	Q9R1Q8	18.59	3	9.05	22.5	7.33	0.0081	1.47
7412	Fructose-bisphosphate aldolase A (ALDOA)	P05064	16.76	4	30.29	39.3	8.09	0.024	2.99
7705	Transketolase (TK)	P40142	10.43	6	25.75	67.6	7.50	0.040	1.52

Fold calculated by dividing average KO protein spot intensity by WT protein spot intensity. *pI=isoelectric point

Table 2 PDQuest and MS/MS results of proteins with significantly altered phosphorylation states in the brain of PINK1 KO mice versus WT mice

Spot	Protein identified	Accession no.	Coverage (%)	Number of identified peptides	Score	MW (kDa)	pI*	*p*-value	Fold increase/ decrease
0008	Calmodulin (CaM)	P62204	42.95	5	51.87	16.8	4.22	0.042	0.418↓
1103	14-3-3 protein epsilon (14-3-3ε)	P62259	51.76	11	81.91	29.2	4.74	0.057	0.480↓
1808	Neurofilament medium polypeptide (NFM)	P08553	19.22	15	116.58	95.9	4.77	0.048	0.275↓
4601	V-type proton ATPase catalytic subunit A (V-ATPaseA)	P50516	32.90	14	111.68	68.3	5.58	0.030	0.313↓
6305	Dual specificity mitogen-activated protein kinase kinase 1 (MAPKK1; MEK1)	P31938	27.23	10	83.53	43.1	6.70	0.025	2.35↑
9201	Mitogen-activated protein kinase 1 (MAPK1)	P63085	16.20	6	35.50	41.2	6.98	0.037	3.39↑

*pI=isoelectric point

Immunoprecipitation and western blot validation experiments

To validate the changes in protein expression and phosphorylation as determined by the PDQuest analysis of the 2-D gels, immunochemistry and 1-D western blotting analysis of *PINK1*$^{(-/-)}$ and WT samples was performed. Figure 3(a) and (b) shows the western blot images from the IP experiments after probing with anti-phosphoserine, anti-phosphothreonine, and anti-phosphotyrosine antibodies, where the immunoprecipitated protein, MAPK1, and CaM, respectively, were

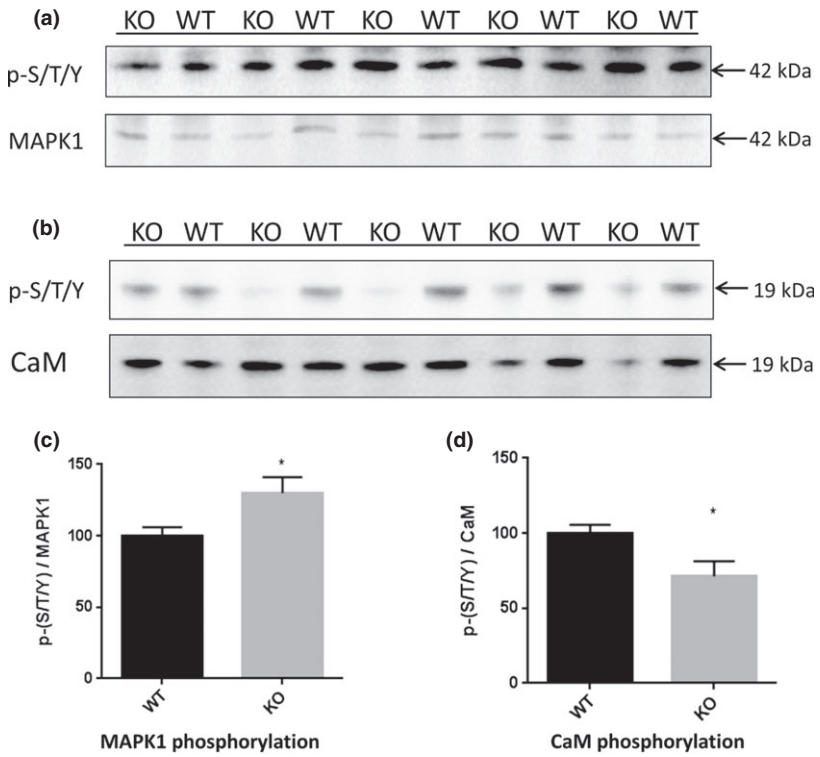

Fig. 3 Western blot validations and corresponding bar graph representations from immunochemistry experiments of (a and c) the significant increase in the phosphorylation of MAPK1 and (b and d) the significant decrease in the phosphorylation of Calmodulin (CaM) in the brains of PINK1 knockout (KO) mice as compared to wild-type (WT) mice using the corresponding immunoprecipitation (IP) antibody as the loading control ($n = 5$, $p < 0.05$). Immunoreactivity with specific antibodies was detected by chemiluminescence. *p < 0.05

used as the loading control. Figure 3(c) and (d) displays the corresponding histogram plot representations of the data. The findings from these analyses confirmed a significant increase in the phosphorylation of MAPK1 ($p = 0.045$) and a decrease in the phosphorylation of CaM ($p = 0.032$) in the brain of *PINK1*$^{(-/-)}$ mice. Figure 4(a) and (b) presents the western blot images of *PINK1*$^{(-/-)}$ and control samples after probing with antibodies for HSP70.2 and ALDOA, respectively, where tubulin was used as the loading control. Figure 4(c) and (d) is the corresponding bar graphs of the results. The results of the western blot analyses confirmed a significant decrease in the expression of HSP70.2 ($p = 0.047$) and a significant increase in the expression of ALDOA ($p = 0.049$) in the *PINK1*$^{(-/-)}$ model. The *p*-values of most of these results are slightly higher than the values obtained from the 2-D proteomic studies. These differences may be attributed to the sensitivity of the Sypro Ruby staining of the 2-D images as compared to the range limitations of the chemiluminescent development of the 1-D western blots.

Discussion

This study focuses on protein expression and phosphorylation changes in the brains of 6-month-old *PINK1*$^{(-/-)}$ mice compared to *PINK1*$^{(+/+)}$ mice. Six-month-old mice were selected based on the observation that at this age *PINK1*$^{(-/-)}$ mice begin to exhibit a PD phenotype, including reduced dopamine levels, providing a model to study early changes occurring in brains with PINK1-related disease progression (Akundi *et al.* 2011). Proteomics studies revealed 29 proteins with significantly altered expression or phosphorylation levels in the brains of PINK1 knockout mice (vs. control mice). These proteins can be subdivided into the following categories that are discussed separately below: cellular signaling, energy metabolism, proteostasis networks, oxidative stress, and neuronal plasticity, neurotransmission, and structure.

Cellular signaling

Regulation of protein phosphorylation status by protein kinases and protein phosphatases is essential in the control of cellular signaling pathways. Ablation of the kinase PINK1 in mice revealed de-regulated downstream phosphorylation events in the brain that may contribute to familial PINK1-related PD pathogenesis. Interestingly, lack of PINK1 is associated with increased phosphorylation of both MAP kinase kinase 1 (MEK1) and its downstream target MAPK1 that modulate vital functions including cell cycle, immunity, autophagy, apoptosis, and cell survival (Dzamko *et al.* 2014). Interestingly, it has been reported that PINK1 deficiency resulted in increased p38 phosphorylation leading to dysfunction of astrocytes (Choi *et al.* 2013). In many neurodegenerative disorders, MAPKs display increased activity and can produce substantial physiological effects with only modest changes in their phosphorylation state (Zhu *et al.* 2003; Di Domenico *et al.* 2011). Phosphorylated MAPKs have been shown to aggregate in the halo region of Lewy bodies and may have an early pathogenic role in PD (Zhu *et al.* 2002).

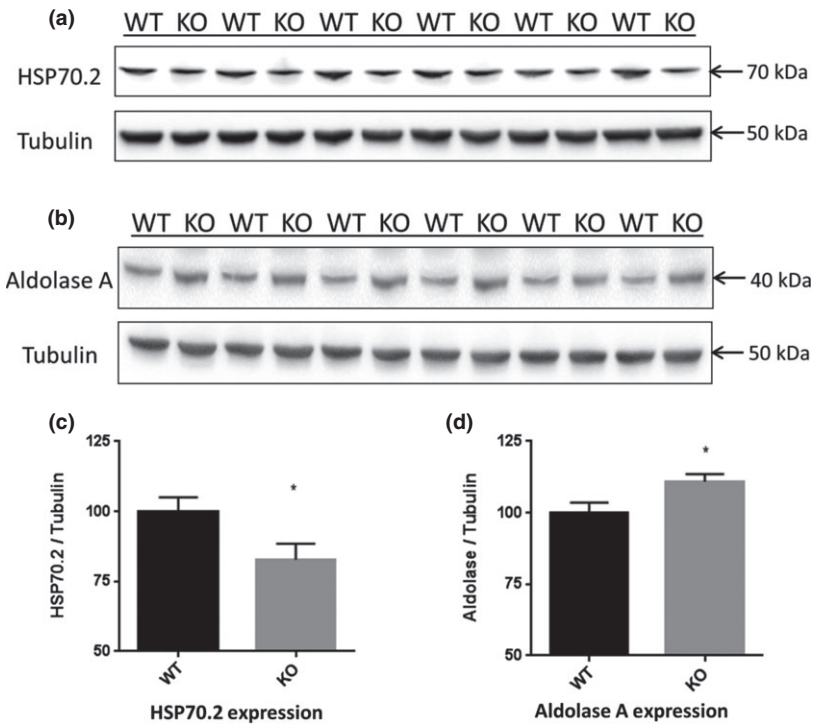

Fig. 4 Western blot validations and corresponding bar graph representations of (a and c) the down-regulation of HSP70.2 and (b and d) the up-regulation of aldolase A (ALDOA) in the brains of PINK1 knockout (KO) mice as compared to wild-type (WT) mice using tubulin as a loading control ($n = 6$, $p < 0.05$). Immunoreactivity with specific antibodies was detected by chemiluminescence. *p < 0.05

Two additional ubiquitous signaling proteins were found to have decreased phosphorylation states in the brains of *PINK1*$^{(-/-)}$ mice: CaM and 14-3-3 protein epsilon. CaM has been identified as a regulator of more than 100 proteins involved in numerous pathways regulating apoptosis, neuronal plasticity, cytoskeletal organization, neurotransmitter release, cellular growth, and proliferation and is a vital regulator of calcium homeostasis (DeLorenzo 1980; Benaim and Villalobo 2002; Xia and Storm 2005). 14-3-3 proteins are known to interact with more than 200 ligands including: kinases, phosphatases, and transmembrane receptors and have been implicated in numerous neurological disorders (Fu *et al.* 2000; Foote and Zhou 2012). Aberrant phosphorylation of either of these identified proteins has the potential to cause a myriad of deleterious downstream effects.

PHB, another ubiquitously expressed pleiotropic modulator of signaling pathways, was found to have significant down-regulated expression in the brains of PINK1 KO mice. One of PHB's more interesting functions is as a chaperone in the assembly of the electron transport chain, and reduced production of ATP has been noted with the loss of PINK1 (Theiss and Sitaraman 2011). In addition, PHB also has been reported to play a defensive role against oxidative stress, and decreased expression of PHB has been correlated with the aging process (Robinson *et al.* 2011), both risk factors or mediators of PD. Further supporting the results of this study, PHB has been shown to be significantly decreased in brains of subjects with PD (Ferrer *et al.* 2007; T. B. Zhou and Qin 2013).

Decreases in expression were also found in APT1 and peptidyl-prolyl cis-trans isomerase A (PPIaseA). APT1 catalyzes the removal of palmitate at CYS residues from the cytosolic surface of membrane proteins (Dekker *et al.* 2010). APT1 regulates protein–protein interactions, cell signaling, membrane localization, subcellular trafficking, vesicle transport, and lysosomal degradation (Tian *et al.* 2012; Kong *et al.* 2013). PPIaseA, also known as cyclophilin A, is a multifunctional protein that catalyzes the cis-trans isomerization at proline residues, playing a role in cellular signaling, inflammation response, and protein trafficking (K. Lang *et al.* 1987; Takahashi *et al.* 1989).

Energy metabolism

A significant number of proteins identified as having altered expression are involved in energy metabolism pathways. We and other groups have shown that PINK1 deficiency impairs mitochondrial respiration, triggering metabolic adaptations including increased glycolysis (Diedrich *et al.* 2011; Yao *et al.* 2012; Akundi *et al.* 2013; Requejo-Aguilar *et al.* 2014). The results of previous discoveries combined with the results of this current investigation provide a more detailed molecular mechanism for the increase in glycolysis noted in PINK1-related PD. Specifically, from this study, we observed an up-regulation of several proteins related to glycolysis in PINK1-deficient mice. These include fructose-bisphosphate ALDOA, ENO2, D-3-phosphoglycerate dehydrogenase (3-PGDH), and transketolase (TK). Not only are ALDOA and ENO2 substrates directly involved in the glycolytic pathway, but ENO2 has been shown to be

neuroprotective when up-regulated in microglial cells (Butterfield and Lange 2009; Hafner *et al.* 2013). Furthermore, 3-PGDH is an oxidoreductase that catalyzes the transition of 3-phosphoglycerate to 3-phosphohydroxypyruvate, the first step in the serine biosynthesis pathway. L-serine is a crucial neurotrophic factor in the CNS as it is a precursor for nucleotides, neurotransmitters, sphingolipids, phosphatidylserine, and L-cysteine (Ren *et al.* 2013). Moreover, the increased levels of neuronal-specific ENO2 and 3-PGDH are likely a cellular stress response to prevent cell death in the absence of PINK1 (presence of mitochondrial dysfunction), consistent with the finding that blocking glycolysis in PINK1-deficient mouse embryonic fibroblasts led to rapid death of these cells (Akundi *et al.* 2013). In addition, TK is an enzyme that catalyzes two key reactions in the pentose phosphate pathway, resulting in the production of glyceraldehyde-3-phosphate and fructose-6-phosphate. Up-regulation of TK provides for more of these essential substrates to be fed into the glycolytic pathway. Moreover, the pentose phosphate pathway provides NADPH, which is needed to reduce oxidized glutathione (GSSG) to reduced glutathione (GSH). Loss of GSH is arguably the earliest neurochemical alteration in PD brain.

DA neurons are reportedly more reliant upon mitochondrial energy metabolism than other types of neurons due, in part, to their reduced mitochondrial reserve (Kingsbury *et al.* 2001; Van Laar and Berman 2013). In PD, depletion of ATP is major factor in the cascade leading to the neurodegeneration of these DA neurons (Mallajosyula *et al.* 2009). Significant decreased levels of cytoplasmic malate dehydrogenase (MDHc), and HPRT were observed in the brain homogenates of PINK1 KO mice. MDHc is a metabolic protein of the malate–aspartate shuttle that aids in the transfer of reducing equivalents of NADH into the mitochondria for consumption by complex I of the electron transport chain. A reduction in this key enzyme would result in impaired mitochondrial ATP synthesis. Moreover, reduced MDHc expression is a plausible contributor to the reduction in complex I activity that is reported in PD and PINK1 model organisms (Gautier *et al.* 2008; Liu *et al.* 2011b), as cytosolic NADH cannot cross the outer mitochondrial membrane without the enzymatic action of MDHc.

HPRT is another metabolic enzyme that is an essential player in the purine salvage pathway for the generation of purine nucleotides (Sculley *et al.* 1992). Increasing nucleotide metabolism is essential for mitochondrial biogenesis fission events to maintain a pool of healthy mitochondria and has been shown to be neuroprotective in PINK1 models of PD (Tufi *et al.* 2014). Interestingly, HPRT deficiency is reported to dysregulate neurogenesis (Guibinga *et al.* 2010), which in adults is responsible for generating new neurons for the olfactory bulb (Altman 1969) and the subgranular zone of the hippocampus (Eriksson *et al.* 1998). Consistent with this observation, PINK1-deficient mice have anosmia (Glasl *et al.* 2012). And, in PD, impaired olfaction occurs 2–7 years before onset of motor symptoms in over 75% of patients (Lang 2011). Furthermore, HPRT knockout mice were shown to have decreased levels of dopamine that correlated with age (Micheli *et al.* 2011). Thus, we suggest that decreased expression of HPRT could quite possibly be a candidate as an early PD biomarker.

Proteostasis networks

Disruption of two intracellular degradation systems, the ubiquitin–proteasome system and autophagy-lysosome pathway, has been shown to play central roles in PD pathology (Lim 2007; Pan *et al.* 2008). Dysregulation of these pathways causes accumulation and aggregation of abnormal proteins and damaged organelles, leading to cellular toxicity, dysfunction and neurodegeneration (Pan *et al.* 2008). Without functional PINK1, mitophagy fails, resulting in accumulated dysfunctional mitochondria and elevated apoptotic rates (Lenzi *et al.* 2012). In this study of PINK1 KO mouse brain, two subunits of V-type proton ATPase were found to be altered in either phosphorylation or expression: V-ATPaseA and V-ATPaseF. V-ATPase is a membrane transport protein whose function is to establish a proton gradient, creating an acidic environment in many intracellular compartments, including lysosomes (Beyenbach and Wieczorek 2006). Previously, we have shown that *C. elegans* expressing mutant α-synuclein and tau have altered V-ATPase and decreased autophagy (Di Domenico *et al.* 2012). Furthermore, when the function of V-ATPase is inhibited, autophagy may become dysfunctional because the acidic environment in lysosomes required for enzymatic hydrolysis cannot be generated (Pan *et al.* 2008). In addition, with diminished lysosomal function, more α-synuclein can accumulate and impair cellular trafficking which may lead to neurodegeneration in PD (Dehay *et al.* 2013). The catalytic subunit A (V-ATPaseA) was found to have decreased phosphorylation. V-ATPaseA is known to be phosphorylated by protein kinase A at Ser-175; and, in liver cells, phosphorylation of subunit A leads to a decreased activity (Alzamora *et al.* 2010), possibly because of decreased binding affinity of ATP to V-ATPaseA. The F subunit of V-type proton ATPase (V-ATPaseF) was identified as having decreased expression, suggesting an overall decrease in vacuolar acidification and autophagy.

Additional proteins involved in the proteostasis network that were found to have significantly decreased expression were as follows: PSA2, HSP70.2, and VDAC-2. PSA2 proteins compose the end rings of the 20S proteasome, an ATP-dependent multi-protein assembly that is known to degrade oxidized proteins (Davies 2001). Hence, elevated oxidatively modified proteins in PD conceivably could be due in part to diminished function of the 20S proteasome. Moreover, as the 20S proteasome comprises the core of the 26S proteasome, the overall protein degradation abilities of

ubiquitin–proteasome system could conceivably be diminished. Consistent with these results, decreased proteasomal function and expression has been noted in PD patients and PD animal models (Bukhatwa *et al.* 2010; Ebrahimi-Fakhari *et al.* 2012; Martins-Branco *et al.* 2012).

HSP70 is an ubiquitously expressed molecular chaperone that mediates the folding of newly translated proteins, stabilizes proteins against aggregation, aids in clathrin mediated endocytosis, exocytosis (including synaptic vesicles) and is an important mediator for relaying targeted proteins to the ubiquitin–proteasome system and autophagy-lysosomal pathways (Meimaridou *et al.* 2009; Alvarez-Erviti *et al.* 2010; Redeker *et al.* 2012). We have previously demonstrated that viral gene transfer of HSP70 protects against toxin-induced DA neuron loss in a sporadic model of PD in mice (Dong *et al.* 2005). In addition, HSP70 suppressed α-synuclein toxicity in a transgenic *Drosophila* model of familial PD (Auluck *et al.* 2002). Therefore, the finding of reduced HSP70 expression is intriguing and is consistent with the notion of an increased vulnerability of DA neurons to mitochondrial and proteotoxic stressors in the absence of PINK1.

VDAC-2 is a mitochondrial membrane porin that opens at low or zero membrane potential, and allows diffusion of small hydrophilic molecules and ions and thus plays a role in mitochondrial metabolic processes (Blachly-Dyson and Forte 2001; Shoshan-Barmatz and Gincel 2003). VDACs are also involved in mitochondrial autophagy, possibly by recruiting Parkin to docking sites in defective mitochondrial membranes, tagging the organelles for degradation by lysosomes (Sun *et al.* 2012). A decrease in the expression of this protein in PD would inhibit the removal of malfunctioning mitochondria, contributing to an increase in cellular detritus and subsequent neuronal dysregulation.

Oxidative stress

Increased levels of reactive oxygen species have been noted in PD and PD model organisms (Jenner 2003; Heeman *et al.* 2011; Di Domenico *et al.* 2012; Varcin *et al.* 2012). Not only does aberrant mitochondrial function and dysfunction of proteostasis networks impact oxidative stress but loss of neurotropic factors contributes as well. Consistent with this observation, two additional neuroprotective enzymes were found in this study to have decreased expression in the brain of the PINK1 KO mouse: CBR3 and cytoplasmic isocitrate dehydrogenase [NADP+] (IDHc). CBR3 is an oxidoreductase that reduces oxidative stress by catalyzing the reduction of carbonyls to their corresponding alcohols (Miura *et al.* 2008). This reduction of oxidative stress-mediated carbonyls leads to the creation of a less toxic species (Oppermann 2007). IDH also plays a defensive role combating oxidative damage as it contains a tagging sequence that can direct damaged proteins to peroxisomes for degradation (Xu *et al.* 2004). In addition, IDHc, utilizing $NADP^+$ as a cofactor, generates NADPH, which noted above is an important cofactor for maintaining reduced GSH, a key antioxidant. Supporting our data, knockdown studies of IDHc in PC12 cell lines demonstrated changes in cellular redox status, increased oxidative damage and apoptotic cell death (Yang and Park 2011). Furthermore, cell lines that expressed lower levels of IDHc were shown to have increased lipid peroxidation, peroxide generation, and oxidative damage to DNA (Lee *et al.* 2002). Consequently, we opine that these proteins may contribute to the oxidative stress observed in PD brain.

Neuronal plasticity, trafficking and structure

Mitochondrial dysfunction is implicated in various neuronal degenerative diseases, leading to decreased neuroplasticity and neurite outgrowth (Cheng *et al.* 2010). Furthermore, PINK1 has previously been reported to be a possible contributor in the regulation of neurite outgrowth, and its deficiency causes dysregulation of this process (Samann *et al.* 2009). In this study, we uncovered a significant decrease in two proteins involved in neurite outgrowth: EF2 and dihydropyrimidase-related protein 2 (DRP2; CRMP2). EF2 mediates ribosomal translocation of peptidyl-tRNA from the A to the P site during protein translation, which has been shown to regulate neurite outgrowth in advancing growth cones (Nairn and Palfrey 1987; Iketani *et al.* 2013). When EF2 is down-regulated or inhibited by EF2 kinase, protein synthesis driving the growth cone is blocked; therefore, formation of new neuronal connections are inhibited (Sutton *et al.* 2007). Furthermore, down-regulation of global protein synthesis has been linked to impaired chaperone and proteasome activity as cells lower protein synthesis when protein folding and/or degradation pathways are impaired to reduce the burden of aggregated and misfolded proteins (van Oosten-Hawle and Morimoto 2014), consistent with the observed decreases in HSP70 and proteasomal subunit expression in this study. Moreover, reducing protein synthesis has shown to be beneficial in a *Drosophila* PINK1 model (Liu and Lu 2010). Thus, while reduced expression of EF2 may affect neurite formation it may also be an adaptive, overall neuroprotective response.

DRP2, also called CRMP2, is a signaling protein that interacts with binding partners and carries out multiple functions, some of which include: neurite outgrowth and retraction, growth cone guidance, kinesin-dependent axonal transport, neurotransmitter release, endocytosis, vesicular cycling, synaptic assembly, Ca^{2+} homeostasis, organization of the dendritic field, and neuronal differentiation (Hensley *et al.* 2011; Khanna *et al.* 2012; Tan *et al.* 2013). Even though overall DRP2 expression decreases with age, higher levels remain in areas of neurogenesis and neuroplasticity (Charrier *et al.* 2003). Previously, DRP2 has been reported to be functionally altered in neurodegenerative disorders, such as Alzheimer disease, prion disease, amyotrophic lateral sclerosis, and PD (De Winter *et al.* 2006; Sultana *et al.*

2006; Shinkai-Ouchi *et al.* 2010; Hensley *et al.* 2011; Dixit *et al.* 2013). It is conceivable that reduced levels of this important neuronal protein affects cytoskeletal organization leading to the decrease in dendritic field and dendritic spine number as reported in PD (Patt *et al.* 1991). Consequently, *PINK1*$^{(-/-)}$ mice deficient in DRP2 would have severely diminished capacity in neuronal repair, migration, neurite elongation, and maintaining neuronal plasticity.

In PD, multiple neuronal networks experience altered neurotransmission, a condition that is exacerbated by α-synuclein over-expression (Barone 2010; Nemani *et al.* 2010). In the *PINK1*$^{(-/-)}$ model in particular, there is a significant reduction in the neurotransmitter dopamine. Decreased expression of V-ATPase in the PINK1 KO mouse is a probable contributor in the breakdown in neurotransmission. Working in conjunction with the H+/neurotransmitter antiporter, V-ATPase assists in the concentration of neurotransmitters into synaptic vesicles (Beyenbach and Wieczorek 2006). Disruption of this process leads to decreased levels of neurotransmitters in the synaptic cleft. Furthermore, synaptic vesicle trafficking at the pre-synaptic cleft is maintained by a cycle of protein complex assembly and disassembly of the SNARE complexes; failure of this cycle can lead to loss of neuronal structure and function(Esposito *et al.* 2012). A central protein involved in this process, vesicle-fusing ATPase, also known as *N*-ethylmaleimide-sensitive fusion protein (NSF), was found in this study to be significantly decreased in the *PINK1*$^{(-/-)}$ brain. NSF is a membrane trafficking chaperone required for intracellular membrane fusion and vesicle-mediated transport (Whiteheart *et al.* 1994; Bomberger *et al.* 2005). Specifically for neurotransmission, NSF facilitates membrane fusion of SNARE complexes (in conjunction with SNAP) for synaptic exocytosis, subsequent disassembly of the complex and mobilization of the reserve neurotransmitter pool (Lin and Scheller 2000; Neuwald 1999; Whiteheart *et al.* 2001), while also promoting re-sensitization of surface receptors on the plasma membrane (Bomberger *et al.* 2005). Knockout of NSF leads to an accumulation of synaptic vesicles at the axon terminals and at the docking site (Whiteheart *et al.* 2001). Consistent with our results and the above notion, PINK1-deficient *Drosophila* neurons show that rapid stimulation of synaptic vesicles is defective (Morais *et al.* 2009).

Loss of neuronal scaffolding is accompanied by decreased expression of structural proteins. In this study, we found two structural proteins to be significantly decreased in the PINK1 KO brain: NFL and ARPC2. NFL is a component in Lewy bodies and a major structural element in neurons, forming the backbone for other neurofilaments (Fuchs and Cleveland 1998). In the substantia nigra of PD subjects, reduced levels of NFL and NFL mRNA were found and correlated with the severity of the disease (Hill *et al.* 1993; Liu *et al.* 2011a). ARPC2 is part of a structural protein complex that plays a role regulating the polymerization and branching of actin filament networks (Gournier *et al.* 2001; Spillane *et al.* 2012). Furthermore, in this study, the phosphorylation state of NFM also was found to be significantly decreased. NFM is a structural protein that supports axonal caliber, and altered levels of NFM phosphorylation affect the function of larger neurofilaments. In addition, phosphorylation of NFM produces inter-filament cross-bridges that increase axonal structure; therefore, a decrease in NFM phosphorylation would be predicted to lead to a decrease in axonal caliber (Mukai *et al.* 1996). Thus, defects in neuronal structural proteins may contribute to the pathogenesis of recessive familial PD.

In conclusion, ablation of PINK1 in mice results in differential expression and altered phosphorylation states of multiple brain proteins with critical functions involved in early changes in cellular signaling pathways, energy metabolism, proteostasis networks, oxidative stress, neurotransmission, and neuronal structural plasticity (Fig. 5). Our findings provide a starting point for future investigations of the impact that these differentially expressed and phosphorylated proteins and their regulated pathways may have on the pathogenesis of PD; particularly the role of potential environmental triggers that interact with mutated PD

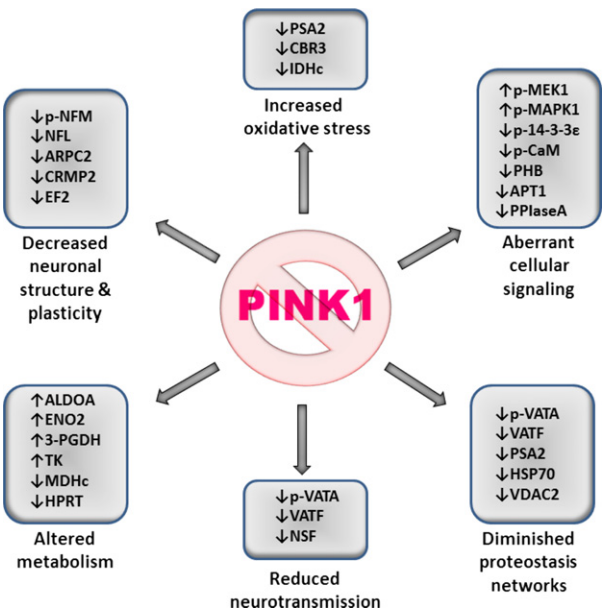

Fig. 5 Schematic diagram summary of expression proteomics and phosphoproteomics profiles of the PINK1 knockout (KO) mouse brain. With the ablation of PINK1, alterations in the phosphoproteome and protein levels were noted in several key proteins associated with: increased oxidative stress, aberrant cellular signaling, altered neuronal structure, decreased synaptic plasticity, reduced neurotransmission, diminished proteostasis networks, and altered metabolism. We hypothesize that such changes contribute to the known alterations in pathology and clinical presentation in Parkinson's disease (PD). See Discussion section for more details.

susceptibility gene. In addition, further studies are required to determine if the proteins identified here may serve as therapeutic targets to interfere with the progression of PD or as part of a panel of potential biomarkers for PD.

Acknowledgments and conflict of interest disclosure

These studies were supported in part by funds from the University of Kentucky Research Challenge Trust Fund. The authors have no conflicts of interest to declare.

All experiments were conducted in compliance with the ARRIVE guidelines.

References

Akundi R. S., Huang Z., Eason J., Pandya J. D., Zhi L., Cass W. A. and Bueler H. (2011) Increased mitochondrial calcium sensitivity and abnormal expression of innate immunity genes precede dopaminergic defects in Pink1-deficient mice. *PLoS ONE* **6**, e16038. doi:10.1371/journal.pone.0016038.

Akundi R. S., Zhi L. and Bueler H. (2012) PINK1 enhances insulin-like growth factor-1-dependent Akt signaling and protection against apoptosis. *Neurobiol. Dis.* **45**, 469–478. doi:10.1016/j.nbd.2011.08.034.

Akundi R. S., Zhi L., Sullivan P. G. and Bueler H. (2013) Shared and cell type-specific mitochondrial defects and metabolic adaptations in primary cells from PINK1-deficient mice. *Neurodegener. Dis.* **12**, 136–149. doi:10.1159/000345689.

Altman J. (1969) Autoradiographic and histological studies of postnatal neurogenesis. IV. Cell proliferation and migration in the anterior forebrain, with special reference to persisting neurogenesis in the olfactory bulb. *J. Comp. Neurol.* **137**, 433–457. doi:10.1002/cne.901370404.

Alvarez-Erviti L., Rodriguez-Oroz M. C., Cooper J. M., Caballero C., Ferrer I., Obeso J. A. and Schapira A. H. (2010) Chaperone-mediated autophagy markers in parkinson disease brains. *Arch. Neurol.* **67**, 1464–1472. doi: 10.1001/archneurol.2010.198

Alzamora R., Thali R. F., Gong F., Smolak C., Li H., Baty C. J. and Pastor-Soler N. M. (2010) PKA regulates vacuolar H + -ATPase localization and activity via direct phosphorylation of the a subunit in kidney cells. *J. Biol. Chem.* **285**, 24676–24685. doi:10.1074/jbc.M110.106278.

Amo T., Sato S., Saiki S., Wolf A. M., Toyomizu M., Gautier C. A., Shen J., Ohta S. and Hattori N. (2011) Mitochondrial membrane potential decrease caused by loss of PINK1 is not due to proton leak, but to respiratory chain defects. *Neurobiol. Dis.* **41**, 111–118. doi: http://dx.doi.org/10.1016/j.nbd.2010.08.027

Anderson J. P., Walker D. E., Goldstein J. M., de Laat R., Banducci K., Caccavello R. J. and Chilcote T. J. (2006) Phosphorylation of Ser-129 is the dominant pathological modification of alpha-synuclein in familial and sporadic Lewy body disease. *J. Biol. Chem.* **281**, 29739–29752. doi:10.1074/jbc.M600933200.

Auluck P. K., Chan H. Y., Trojanowski J. Q., Lee V. M. and Bonini N. M. (2002) Chaperone suppression of alpha-synuclein toxicity in a Drosophila model for Parkinson's disease. *Science* **295**, 865–868. doi:10.1126/science.1067389.

Barone P. (2010) Neurotransmission in Parkinson's disease: beyond dopamine. *Eur. J. Neurol.* **17**, 364–376. doi:10.1111/j.1468-1331.2009.02900.x.

Benaim G. and Villalobo A. (2002) Phosphorylation of calmodulin. Functional implications. *Eur. J. Biochem.* **269**, 3619–3631.

Beyenbach K. W. and Wieczorek H. (2006) The V-type H+ ATPase: molecular structure and function, physiological roles and regulation. *J. Exp. Biol.* **209**, 577–589. doi:10.1242/jeb.02014.

Blachly-Dyson E. and Forte M. (2001) VDAC Channels. *IUBMB Life* **52**, 113–118. doi:10.1080/15216540152845902.

Bomberger J. M., Parameswaran N., Hall C. S., Aiyar N. and Spielman W. S. (2005) Novel function for receptor activity-modifying proteins (RAMPs) in post-endocytic receptor trafficking. *J. Biol. Chem.* **280**, 9297–9307. doi:10.1074/jbc.M413786200.

Bonifati V. (2012) Autosomal recessive parkinsonism. *Parkinsonism Relat. Disord.* **18**(Suppl 1), S4–S6. doi:10.1016/S1353-8020(11)70004-9.

Bonifati V., Rohe C. F., Breedveld G. J. *et al.*; Italian Parkinson Genetics Network (2005) Early-onset parkinsonism associated with PINK1 mutations: frequency, genotypes, and phenotypes. *Neurology* **65**, 87–95. doi: 10.1212/01.wnl.0000167546.39375.82

Braak H., Tredici K. D., Rüb U., deVos R. A. I., Jansen Steur E. N. H. and Braak E. (2003) Staging of brain pathology related to sporadic Parkinson's disease. *Neurobiol. Aging* **24**, 197–211. doi: http://dx.doi.org/10.1016/S0197-4580(02)00065-9

Bueler H. (2009) Impaired mitochondrial dynamics and function in the pathogenesis of Parkinson's disease. *Exp. Neurol.* **218**, 235–246. doi:10.1016/j.expneurol.2009.03.006.

Bukhatwa S., Zeng B.-Y., Rose S. and Jenner P. (2010) A comparison of changes in proteasomal subunit expression in the substantia nigra in Parkinson's disease, multiple system atrophy and progressive supranuclear palsy. *Brain Res.* **1326**, 174–183. doi: http://dx.doi.org/10.1016/j.brainres.2010.02.045

Butterfield D. A. and Lange M. L. (2009) Multifunctional roles of enolase in Alzheimer's disease brain: beyond altered glucose metabolism. *J. Neurochem.* **111**, 915–933. doi:10.1111/j.1471-4159.2009.06397.x.

Charrier E., Reibel S., Rogemond V., Aguera M., Thomasset N. and Honnorat J. (2003) Collapsin response mediator proteins (CRMPs): involvement in nervous system development and adult neurodegenerative disorders. *Mol. Neurobiol.* **28**, 51–64. doi:10.1385/MN:28:1:51.

Chaudhuri K. R., Healy D. G. and Schapira A. H.;National Institute for Clinical Exellence (2006) Non-motor symptoms of Parkinson's disease: diagnosis and management. *Lancet Neurol.* **5**, 235–245. doi: 10.1016/S1474-4422(06)70373-8

Cheng A., Hou Y. and Mattson M. P. (2010) Mitochondria and neuroplasticity. *ASN Neuro* **2**, e00045. doi:10.1042/an20100019.

Choi I., Kim J., Jeong H. K., Kim B., Jou I., Park S. M. and Joe E. H. (2013) PINK1 deficiency attenuates astrocyte proliferation through mitochondrial dysfunction, reduced AKT and increased p38 MAPK activation, and downregulation of EGFR. *Glia* **61**, 800–812. doi:10.1002/glia.22475.

Davies K. J. A. (2001) Degradation of oxidized proteins by the 20S proteasome. *Biochimie* **83**, 301–310. doi: http://dx.doi.org/10.1016/S0300-9084(01)01250-0

De Winter F., Vo T., Stam F. J., Wisman L. A., Bar P. R., Niclou S. P. and Verhaagen J. (2006) The expression of the chemorepellent Semaphorin 3A is selectively induced in terminal Schwann cells of a subset of neuromuscular synapses that display limited anatomical plasticity and enhanced vulnerability in motor neuron disease. *Mol. Cell Neurosci.* **32**, 102–117. doi:10.1016/j.mcn.2006.03.002.

Deas E., Plun-Favreau H., Gandhi S., Desmond H., Kjaer S., Loh S. H. and Wood N. W. (2011) PINK1 cleavage at position A103 by the mitochondrial protease PARL. *Hum. Mol. Genet.* **20**, 867–879. doi:10.1093/hmg/ddq526.

Dehay B., Martinez-Vicente M., Caldwell G. A., Caldwell K. A., Yue Z., Cookson M. R. and Bezard E. (2013) Lysosomal impairment in

Parkinson's disease. *Mov. Disord.* **28**, 725–732. doi:10.1002/mds.25462.

Dekker F. J., Rocks O., Vartak N., Menninger S., Hedberg C., Balamurugan R. and Waldmann H. (2010) Small-molecule inhibition of APT1 affects Ras localization and signaling. *Nat. Chem. Biol.* **6**, 449–456. doi:10.1038/nchembio.362.

DeLorenzo R. J. (1980) Role of calmodulin in neurotransmitter release and synaptic function. *Ann. N. Y. Acad. Sci.* **356**, 92–109.

Di Domenico F., Sultana R., Barone E., Perluigi M., Cini C., Mancuso C. and Butterfield D. A. (2011) Quantitative proteomics analysis of phosphorylated proteins in the hippocampus of Alzheimer's disease subjects. *J. Proteomics.* **74**, 1091–1103. doi:10.1016/j.jprot.2011.03.033.

Di Domenico F., Sultana R., Ferree A., Smith K., Barone E., Perluigi M. and Butterfield D. A. (2012) Redox proteomics analyses of the influence of co-expression of wild-type or mutated LRRK2 and Tau on C. elegans protein expression and oxidative modification: relevance to Parkinson disease. *Antioxid. Redox Signal.* **17**, 1490–1506. doi:10.1089/ars.2011.4312.

Diedrich M., Kitada T., Nebrich G., Koppelstaetter A., Shen J., Zabel C. and Mao L. (2011) Brain region specific mitophagy capacity could contribute to selective neuronal vulnerability in Parkinson's disease. *Proteome Sci.* **9**, 59. doi:10.1186/1477-5956-9-59.

Dixit A., Srivastava G., Verma D., Mishra M., Singh P. K., Prakash O. and Singh M. P. (2013) Minocycline, levodopa and MnTMPyP induced changes in the mitochondrial proteome profile of MPTP and maneb and paraquat mice models of Parkinson's disease. *Biochim. Biophys. Acta* **1832**, 1227–1240. doi:10.1016/j.bbadis.2013.03.019.

Dong Z., Wolfer D. P., Lipp H. P. and Bueler H. (2005) Hsp70 gene transfer by adeno-associated virus inhibits MPTP-induced nigrostriatal degeneration in the mouse model of Parkinson disease. *Mol. Ther.* **11**, 80–88. doi:10.1016/j.ymthe.2004.09.007.

Dzamko N., Zhou J., Huang Y. and Halliday G. M. (2014) Parkinson's disease-implicated kinases in the brain; insights into disease pathogenesis. *Front. Mol. Neurosci.* **7**, 57. doi:10.3389/fnmol.2014.00057.

Ebrahimi-Fakhari D., Wahlster L. and McLean P. (2012) Protein degradation pathways in Parkinson's disease: curse or blessing. *Acta Neuropathol.* **124**, 153–172. doi:10.1007/s00401-012-1004-6.

Eriksson P. S., Perfilieva E., Bjork-Eriksson T., Alborn A. M., Nordborg C., Peterson D. A. and Gage F. H. (1998) Neurogenesis in the adult human hippocampus. *Nat. Med.* **4**, 1313–1317. doi:10.1038/3305.

Esposito G., Ana Clara F. and Verstreken P. (2012) Synaptic vesicle trafficking and Parkinson's disease. *Dev. Neurobiol.* **72**, 134–144. doi:10.1002/dneu.20916.

Exner N., Treske B., Paquet D. *et al.* (2007) Loss-of-function of human PINK1 results in mitochondrial pathology and can be rescued by parkin. *J. Neurosci.* **27**, 12413–12418. doi:10.1523/JNEUROSCI.0719-07.2007.

Fedorowicz M. A., de Vries-Schneider R. L., Rub C., Becker D., Huang Y., Zhou C., Alessi Wolken D. M., Voos W., Liu Y. and Przedborski S. (2014) Cytosolic cleaved PINK1 represses Parkin translocation to mitochondria and mitophagy. *EMBO Rep.* **15**, 86–93. doi: 10.1002/embr.201337294

Ferrer I., Perez E., Dalfo E. and Barrachina M. (2007) Abnormal levels of prohibitin and ATP synthase in the substantia nigra and frontal cortex in Parkinson's disease. *Neurosci. Lett.* **415**, 205–209. doi:10.1016/j.neulet.2007.01.026.

Foote M. and Zhou Y. (2012) 14-3-3 proteins in neurological disorders. *Int. J. Biochem. Mol. Biol.* **3**, 152–164.

Fu H., Subramanian R. R. and Masters S. C. (2000) 14-3-3 proteins: structure, function, and regulation. *Annu. Rev. Pharmacol. Toxicol.* **40**, 617–647. doi:10.1146/annurev.pharmtox.40.1.617.

Fuchs E. and Cleveland D. W. (1998) A structural scaffolding of intermediate filaments in health and disease. *Science* **279**, 514–519.

Gasser T., Hardy J. and Mizuno Y. (2011) Milestones in PD genetics. *Mov. Disord.* **26**, 1042–1048. doi:10.1002/mds.23637.

Gautier C. A., Kitada T. and Shen J. (2008) Loss of PINK1 causes mitochondrial functional defects and increased sensitivity to oxidative stress. *Proc. Natl Acad. Sci. USA* **105**, 11364–11369. doi:10.1073/pnas.0802076105.

Gautier C. A., Giaime E., Caballero E., Nunez L., Song Z., Chan D., Villalobos C. and Shen J. (2012) Regulation of mitochondrial permeability transition pore by PINK1. *Mol. Neurodegener.* **7**, 22. doi:10.1186/1750-1326-7-22.

Glasl L., Kloos K., Giesert F. *et al.* (2012) Pink1-deficiency in mice impairs gait, olfaction and serotonergic innervation of the olfactory bulb. *Exp. Neurol.* **235**, 214–227. doi:10.1016/j.expneurol.2012.01.002.

Gournier H., Goley E. D., Niederstrasser H., Trinh T. and Welch M. D. (2001) Reconstitution of human Arp2/3 complex reveals critical roles of individual subunits in complex structure and activity. *Mol. Cell* **8**, 1041–1052. doi: http://dx.doi.org/10.1016/S1097-2765(01)00393-8

Guibinga G. H., Hsu S. and Friedmann T. (2010) Deficiency of the housekeeping gene hypoxanthine-guanine phosphoribosyltransferase (HPRT) dysregulates neurogenesis. *Mol. Ther.* **18**, 54–62. doi:10.1038/mt.2009.178.

Hafner A., Glavan G., Obermajer N., Živin M., Schliebs R. and Kos J. (2013) Neuroprotective role of γ-enolase in microglia in a mouse model of Alzheimer's disease is regulated by cathepsin X. *Aging Cell*, **12**, 604–614. doi:10.1111/acel.12093.

Haque M. E., Thomas K. J., D'Souza C., Callaghan S., Kitada T., Slack R. S., Fraser P., Cookson M. R., Tandon A. and Park D. S. (2008) Cytoplasmic Pink1 activity protects neurons from dopaminergic neurotoxin MPTP. *Proc. Natl Acad. Sci. USA* **105**, 1716–1721. doi:10.1073/pnas.0705363105.

Hauser D. N. and Hastings T. G. (2013) Mitochondrial dysfunction and oxidative stress in Parkinson's disease and monogenic parkinsonism. *Neurobiol. Dis.* **51**, 35–42. doi:10.1016/j.nbd.2012.10.011.

Heeman B., Van den Haute C., Aelvoet S. A. *et al.* (2011) Depletion of PINK1 affects mitochondrial metabolism, calcium homeostasis and energy maintenance. *J. Cell Sci.* **124**, 1115–1125. doi:10.1242/jcs.078303.

Henchcliffe C. and Beal M. F. (2008) Mitochondrial biology and oxidative stress in Parkinson disease pathogenesis. *Nat. Clin. Pract. Neurol.* **4**, 600–609. doi:10.1038/ncpneuro0924.

Hensley K., Venkova K., Christov A., Gunning W. and Park J. (2011) Collapsin response mediator protein-2: an emerging pathologic feature and therapeutic target for neurodisease indications. *Mol. Neurobiol.* **43**, 180–191. doi:10.1007/s12035-011-8166-4.

Hill W. D., Arai M., Cohen J. A. and Trojanowski J. Q. (1993) Neurofilament mRNA is reduced in Parkinson's disease substantia nigra pars compacta neurons. *J. Comp. Neurol.* **329**, 328–336. doi:10.1002/cne.903290304.

Iketani M., Iizuka A., Sengoku K. *et al.* (2013) Regulation of neurite outgrowth mediated by localized phosphorylation of protein translational factor eEF2 in growth cones. *Dev. Neurobiol.* **73**, 230–246. doi:10.1002/dneu.22058.

Jankovic J. (2008) Parkinson's disease: clinical features and diagnosis. *J. Neurol. Neurosurg. Psychiatry* **79**, 368–376. doi:10.1136/jnnp.2007.131045.

Jenner P. (2003) Oxidative stress in Parkinson's disease. *Ann. Neurol.* **53**(Suppl 3), S26–S36; discussion S36-28. doi: 10.1002/ana.10483

Jin S. M. and Youle R. J. (2012) PINK1- and Parkin-mediated mitophagy at a glance. *J. Cell Sci.* **125**, 795–799. doi:10.1242/jcs.093849.

Kazlauskaite A., Kondapalli C., Gourlay R., Campbell D. G., Ritorto M. S., Hofmann K., Alessi D. R., Knebel A., Trost M. and Muqit M. M. (2014) Parkin is activated by PINK1-dependent phosphorylation of ubiquitin at Ser65. *Biochem. J.* **460**, 127–139. doi:10.1042/BJ20140334.

Khanna R., Wilson S. M., Brittain J. M., Weimer J., Sultana R., Butterfield A. and Hensley K. (2012) Opening Pandora's jar: a primer on the putative roles of CRMP2 in a panoply of neurodegenerative, sensory and motor neuron, and central disorders. *Future Neurol.* **7**, 749–771. doi:10.2217/FNL.12.68.

Kingsbury A. E., Cooper M., Schapira A. H. and Foster O. J. (2001) Metabolic enzyme expression in dopaminergic neurons in Parkinson's disease: an in situ hybridization study. *Ann. Neurol.* **50**, 142–149.

Koh H. and Chung J. (2012) PINK1 as a molecular checkpoint in the maintenance of mitochondrial function and integrity. *Mol. Cells* **34**, 7–13. doi:10.1007/s10059-012-0100-8.

Kong E., Peng S., Chandra G., Sarkar C., Zhang Z., Bagh M. B. and Mukherjee A. B. (2013) Dynamic palmitoylation links cytosol-membrane shuttling of acyl-protein thioesterase-1 and acyl-protein thioesterase-2 with that of proto-oncogene H-ras product and growth-associated protein-43. *J. Biol. Chem.* **288**, 9112–9125. doi:10.1074/jbc.M112.421073.

Lang A. E. (2011) A critical appraisal of the premotor symptoms of Parkinson's disease: potential usefulness in early diagnosis and design of neuroprotective trials. *Mov. Disord.* **26**, 775–783. doi:10.1002/mds.23609.

Lang K., Schmid F. X. and Fischer G. (1987) Catalysis of protein folding by prolyl isomerase. *Nature* **329**, 268–270. doi:10.1038/329268a0.

Lee S. M., Koh H.-J., Park D.-C., Song B. J., Huh T.-L. and Park J.-W. (2002) Cytosolic NADP+-dependent isocitrate dehydrogenase status modulates oxidative damage to cells. *Free Radic. Biol. Med.* **32**, 1185–1196. doi: http://dx.doi.org/10.1016/S0891-5849(02)00815-8

Lenzi P., Marongiu R., Falleni A., Gelmetti V., Busceti C. L., Michiorri S., Valente E. M. and Fornai F. (2012) A subcellular analysis of genetic modulation of PINK1 on mitochondrial alterations, autophagy and cell death. *Arch. Ital. Biol.* **150**, 194–217. doi:10.4449/aib.v150i2/3.1417.

Liang C. L., Wang T. T., Luby-Phelps K. and German D. C. (2007) Mitochondria mass is low in mouse substantia nigra dopamine neurons: implications for Parkinson's disease. *Exp. Neurol.* **203**, 370–380. doi:10.1016/j.expneurol.2006.08.015.

Lim K. L. (2007) Ubiquitin-proteasome system dysfunction in Parkinson's disease: current evidence and controversies. *Expert Rev. Proteomics* **4**, 769–781. doi:10.1586/14789450.4.6.769.

Lin W. and Kang U. J. (2008) Characterization of PINK1 processing, stability, and subcellular localization. *J. Neurochem.* **106**, 464–474. doi:10.1111/j.1471-4159.2008.05398.x.

Lin R. C. and Scheller R. H. (2000) Mechanisms of synaptic vesicle exocytosis. *Annu. Rev. Cell Dev. Biol.* **16**, 19–49. doi:10.1146/annurev.cellbio.16.1.19.

Liu S. and Lu B. (2010) Reduction of protein translation and activation of autophagy protect against PINK1 pathogenesis in Drosophila melanogaster. *PLoS Genet.* **6**, e1001237. doi:10.1371/journal.pgen.1001237.

LiuQ Q., Xie F., Alvarado-Diaz A., Smith M. A., Moreira P. I., Zhu X. and Perry G. (2011a) Neurofilamentopathy in neurodegenerative diseases. *Open Neurol. J.* **5**, 58–62. doi:10.2174/1874205X01105010058.

Liu W., Acin-Perez R., Geghman K. D., Manfredi G., Lu B. and Li C. (2011b) Pink1 regulates the oxidative phosphorylation machinery via mitochondrial fission. *Proc. Natl Acad. Sci. USA* **108**, 12920–12924. doi:10.1073/pnas.1107332108.

Mallajosyula J. K., Chinta S. J., Rajagopalan S., Nicholls D. G. and Andersen J. K. (2009) Metabolic control analysis in a cellular model of elevated MAO-B: relevance to Parkinson's disease. *Neurotox. Res.* **16**, 186–193. doi:10.1007/s12640-009-9032-2.

Martins-Branco D., Esteves A. R., Santos D., Arduino D. M., Swerdlow R. H., Oliveira C. R., Januario C. and Cardoso S. M. (2012) Ubiquitin proteasome system in Parkinson's disease: a keeper or a witness? *Exp. Neurol.* **238**, 89–99. doi: http://dx.doi.org/10.1016/j.expneurol.2012.08.008

Matsuda N., Sato S., Shiba K. *et al.* (2010) PINK1 stabilized by mitochondrial depolarization recruits Parkin to damaged mitochondria and activates latent Parkin for mitophagy. *J. Cell Biol.* **189**, 211–221. doi:10.1083/jcb.200910140.

Meimaridou E., Gooljar S. B. and Chapple J. P. (2009) From hatching to dispatching: the multiple cellular roles of the Hsp70 molecular chaperone machinery. *J. Mol. Endocrinol.* **42**, 1–9. doi:10.1677/jme-08-0116.

Meissner C., Lorenz H., Weihofen A., Selkoe D. J. and Lemberg M. K. (2011) The mitochondrial intramembrane protease PARL cleaves human Pink1 to regulate Pink1 trafficking. *J. Neurochem.* **117**, 856–867. doi:10.1111/j.1471-4159.2011.07253.x.

Micheli V., Camici M., Tozzi M. G., Ipata P. L., Sestini S., Bertelli M. and Pompucci G. (2011) Neurological disorders of purine and pyrimidine metabolism. *Curr. Top. Med. Chem.* **11**, 923–947.

Miura T., Nishinaka T. and Terada T. (2008) Different functions between human monomeric carbonyl reductase 3 and carbonyl reductase 1. *Mol. Cell. Biochem.* **315**, 113–121. doi:10.1007/s11010-008-9794-5.

Morais V. A., Verstreken P., Roethig A. *et al.* (2009) Parkinson's disease mutations in PINK1 result in decreased Complex I activity and deficient synaptic function. *EMBO Mol. Med.* **1**, 99–111. doi:10.1002/emmm.200900006.

Morais V. A., Haddad D., Craessaerts K. *et al.* (2014) PINK1 loss-of-function mutations affect mitochondrial complex I activity via NdufA10 ubiquinone uncoupling. *Science* **344**, 203–207. doi:10.1126/science.1249161.

Mukai H., Toshimori M., Shibata H., Kitagawa M., Shimakawa M., Miyahara M., Sunakawa H. and Ono Y. (1996) PKN associates and phosphorylates the head-rod domain of neurofilament protein. *J. Biol. Chem.* **271**, 9816–9822.

Murata H., Sakaguchi M., Jin Y., Sakaguchi Y., Futami J., Yamada H., Kataoka K. and Huh N. H. (2011) A new cytosolic pathway from a Parkinson disease-associated kinase, BRPK/PINK1: activation of AKT via mTORC2. *J. Biol. Chem.* **286**, 7182–7189. doi:10.1074/jbc.M110.179390.

Nairn A. C. and Palfrey H. C. (1987) Identification of the major Mr 100,000 substrate for calmodulin-dependent protein kinase III in mammalian cells as elongation factor-2. *J. Biol. Chem.* **262**, 17299–17303.

Narendra D. P., Jin S. M., Tanaka A., Suen D. F., Gautier C. A., Shen J., Cookson M. R. and Youle R. J. (2010) PINK1 is selectively stabilized on impaired mitochondria to activate Parkin. *PLoS Biol.* **8**, e1000298. doi:10.1371/journal.pbio.1000298.

Nemani V. M., Lu W., Berge V., Nakamura K., Onoa B., Lee M. K., Chaudhry F. A., Nicoll R. A. and Edwards R. H. (2010) Increased expression of a-synuclein reduces neurotransmitter release by inhibiting synaptic vesicle reclustering after endocytosis. *Neuron* **65**, 66–79. doi: http://dx.doi.org/10.1016/j.neuron.2009.12.023

Neuwald A. F. (1999) The hexamerization domain of N-ethylmaleimide-sensitive factor: structural clues to chaperone function. *Structure* **7**, R19–R23.

van Oosten-Hawle P. and Morimoto R. I. (2014) Organismal proteostasis: role of cell-nonautonomous regulation and transcellular chaperone signaling. *Genes Dev.* **28**, 1533–1543. doi:10.1101/gad.241125.114.

Oppermann U. (2007) Carbonyl reductases: the complex relationships of mammalian carbonyl- and quinone-reducing enzymes and their role in physiology. *Annu. Rev. Pharmacol. Toxicol.* **47**, 293–322. doi:10.1146/annurev.pharmtox.47.120505.105316.

Pan T., Kondo S., Le W. and Jankovic J. (2008) The role of autophagy-lysosome pathway in neurodegeneration associated with Parkinson's disease. *Brain* **131**, 1969–1978. doi:10.1093/brain/awm318.

Park J., Lee S. B., Lee S. *et al.* (2006) Mitochondrial dysfunction in Drosophila PINK1 mutants is complemented by parkin. *Nature* **441**, 1157–1161. doi:10.1038/nature04788.

Patt S., Gertz H. J., Gerhard L. and Cervos-Navarro J. (1991) Pathological changes in dendrites of substantia nigra neurons in Parkinson's disease: a Golgi study. *Histol. Histopathol.* **6**, 373–380.

Pilsl A. and Winklhofer K. F. (2012) Parkin, PINK1 and mitochondrial integrity: emerging concepts of mitochondrial dysfunction in Parkinson's disease. *Acta Neuropathol.* **123**, 173–188. doi:10.1007/s00401-011-0902-3.

Redeker V., Pemberton S., Bienvenut W., Bousset L. and Melki R. (2012) Identification of protein interfaces between alpha-synuclein, the principal component of Lewy bodies in Parkinson disease, and the molecular chaperones human Hsc70 and the yeast Ssa1p. *J. Biol. Chem.* **287**, 32630–32639. doi:10.1074/jbc.M112.387530.

Ren T. J., Qiang R., Jiang Z. L., Wang G. H., Sun L., Jiang R., Zhao G. W. and Han L. Y. (2013) Improvement in regional CBF by L-serine contributes to its neuroprotective effect in rats after focal cerebral ischemia. *PLoS ONE* **8**, e67044. doi: 10.1371/journal.pone.0067044

Requejo-Aguilar R., Lopez-Fabuel I., Fernandez E., Martins L. M., Almeida A. and Bolanos J. P. (2014) PINK1 deficiency sustains cell proliferation by reprogramming glucose metabolism through HIF1. *Nat. Commun.* **5**, 4514. doi:10.1038/ncomms5514.

Robinson R. A., Joshi G., Huang Q., Sultana R., Baker A. S., Cai J., Pierce W., St Clair D. K., Markesbery W. R. and Butterfield D. A. (2011) Proteomic analysis of brain proteins in APP/PS-1 human double mutant knock-in mice with increasing amyloid beta-peptide deposition: insights into the effects of in vivo treatment with N-acetylcysteine as a potential therapeutic intervention in mild cognitive impairment and Alzheimer's disease. *Proteomics* **11**, 4243–4256. doi:10.1002/pmic.201000523.

Samann J., Hegermann J., von Gromoff E., Eimer S., Baumeister R. and Schmidt E. (2009) Caenorhabditits elegans LRK-1 and PINK-1 act antagonistically in stress response and neurite outgrowth. *J. Biol. Chem.* **284**, 16482–16491. doi:10.1074/jbc.M808255200.

Sculley D. G., Dawson P. A., Emmerson B. T. and Gordon R. B. (1992) A review of the molecular basis of hypoxanthine-guanine phosphoribosyltransferase (HPRT) deficiency. *Hum. Genet.* **90**, 195–207.

Shinkai-Ouchi F., Yamakawa Y., Hara H., Tobiume M., Nishijima M., Hanada K. and Hagiwara K. (2010) Identification and structural analysis of C-terminally truncated collapsin response mediator protein-2 in a murine model of prion diseases. *Proteome Sci.* **8**, 53. doi:10.1186/1477-5956-8-53.

Shoshan-Barmatz V. and Gincel D. (2003) The voltage-dependent anion channel. *Cell Biochem. Biophys.* **39**, 279–292. doi:10.1385/cbb:39:3:279.

Smith P. K., Krohn R. I., Hermanson G. T., Mallia A. K., Gartner F. H., Provenzano M. D., Fujimoto E. K., Goeke N. M., Olson B. J. and Klenk D. C. (1985) Measurement of protein using bicinchoninic acid. *Anal. Biochem.* **150**, 76–85.

Spillane M., Ketschek A., Donnelly C. J., Pacheco A., Twiss J. L. and Gallo G. (2012) Nerve growth factor-induced formation of axonal filopodia and collateral branches involves the intra-axonal synthesis of regulators of the actin-nucleating Arp2/3 complex. *J. Neurosci.* **32**, 17671–17689. doi:10.1523/JNEUROSCI.1079-12.2012.

Sultana R., Boyd-Kimball D., Poon H. F., Cai J., Pierce W. M., Klein J. B., Merchant M., Markesbery W. R. and Butterfield D. A. (2006) Redox proteomics identification of oxidized proteins in Alzheimer's disease hippocampus and cerebellum: an approach to understand pathological and biochemical alterations in AD. *Neurobiol. Aging* **27**, 1564–1576. doi:10.1016/j.neurobiolaging.2005.09.021.

Sultana R., Boyd-Kimball D., Cai J., Pierce W. M., Klein J. B., Merchant M. and Butterfield D. A. (2007) Proteomics analysis of the Alzheimer's disease hippocampal proteome. *J. Alzheimers Dis.* **11**, 153–164.

Sun Y., Vashisht A. A., Tchieu J., Wohlschlegel J. A. and Dreier L. (2012) Voltage-dependent anion channels (VDACs) recruit Parkin to defective mitochondria to promote mitochondrial autophagy. *J. Biol. Chem.* **287**, 40652–40660. doi:10.1074/jbc.M112.419721.

Surmeier D. J., Guzman J. N., Sanchez-Padilla J. and Schumacker P. T. (2011) The role of calcium and mitochondrial oxidant stress in the loss of substantia nigra pars compacta dopaminergic neurons in Parkinson's disease. *Neuroscience* **198**, 221–231. doi:10.1016/j.neuroscience.2011.08.045.

Sutton M. A., Taylor A. M., Ito H. T., Pham A. and Schuman E. M. (2007) Postsynaptic decoding of neural activity: eEF2 as a biochemical sensor coupling miniature synaptic transmission to local protein synthesis. *Neuron* **55**, 648–661. doi: http://dx.doi.org/10.1016/j.neuron.2007.07.030

Takahashi N., Hayano T. and Suzuki M. (1989) Peptidyl-prolyl cis-trans isomerase is the cyclosporin A-binding protein cyclophilin. *Nature* **337**, 473–475. doi:10.1038/337473a0.

Tan M., Ma S., Huang Q., Hu K., Song B. and Li M. (2013) GSK-3alpha/beta-mediated phosphorylation of CRMP-2 regulates activity-dependent dendritic growth. *J. Neurochem.* **125**, 685–697. doi:10.1111/jnc.12230.

Tansey M. G. and Goldberg M. S. (2010) Neuroinflammation in Parkinson's disease: its role in neuronal death and implications for therapeutic intervention. *Neurobiol. Dis.* **37**, 510–518. doi:10.1016/j.nbd.2009.11.004.

Theiss A. L. and Sitaraman S. V. (2011) The role and therapeutic potential of prohibitin in disease. *Biochim. Biophys. Acta* **1813**, 1137–1143. doi:10.1016/j.bbamcr.2011.01.033.

Thongboonkerd V., McLeish K. R., Arthur J. M. and Klein J. B. (2002) Proteomic analysis of normal human urinary proteins isolated by acetone precipitation or ultracentrifugation. *Kidney Int.* **62**, 1461–1469. doi:10.1111/j.1523-1755.2002.kid565.x.

Tian L., McClafferty H., Knaus H. G., Ruth P. and Shipston M. J. (2012) Distinct acyl protein transferases and thioesterases control surface expression of calcium-activated potassium channels. *J. Biol. Chem.* **287**, 14718–14725. doi:10.1074/jbc.M111.335547.

Tufi R., Gandhi S., de Castro I. P. *et al.* (2014) Enhancing nucleotide metabolism protects against mitochondrial dysfunction and neurodegeneration in a PINK1 model of Parkinson's disease. *Nat. Cell Biol.* **16**, 157–166. doi:10.1038/ncb2901.

Twelves D., Perkins K. S. M. and Counsell C. (2003) Systematic review of incidence studies of Parkinson's disease. *Mov. Disord.* **18**, 19–31. doi:10.1002/mds.10305.

Valente E. M., Abou-Sleiman P. M., Caputo V. *et al.* (2004) Hereditary early-onset Parkinson's disease caused by mutations in PINK1. *Science* **304**, 1158–1160. doi:10.1126/science.1096284.

Van Laar V. S. and Berman S. B. (2013) The interplay of neuronal mitochondrial dynamics and bioenergetics: implications for Parkinson's disease. *Neurobiol. Dis.* **51**, 43–55. doi:10.1016/j.nbd.2012.05.015.

Varcin M., Bentea E., Michotte Y. and Sarre S. (2012) Oxidative stress in genetic mouse models of Parkinson's disease. *Oxid. Med. Cell. Longev.* **2012**, 624925. doi:10.1155/2012/624925.

Whiteheart S. W., Rossnagel K., Buhrow S. A., Brunner M., Jaenicke R. and Rothman J. E. (1994) N-ethylmaleimide-sensitive fusion protein: a trimeric ATPase whose hydrolysis of ATP is required for membrane fusion. *J. Cell Biol.* **126**, 945–954.

Whiteheart S. W., Schraw T. and Matveeva E. A. (2001) N-Ethylmaleimide sensitive factor NSF structure and function. *Int. Rev. Cytol.* **207**, 71–112.

Xia Z. and Storm D. R. (2005) The role of calmodulin as a signal integrator for synaptic plasticity. *Nat. Rev. Neurosci.* **6**, 267–276. doi:10.1038/nrn1647.

Xu X., Zhao J., Xu Z., Peng B., Huang Q., Arnold E. and Ding J. (2004) Structures of human cytosolic NADP-dependent isocitrate dehydrogenase reveal a novel self-regulatory mechanism of activity. *J. Biol. Chem.* **279**, 33946–33957. doi:10.1074/jbc.M404298200.

Yamano K. and Youle R. J. (2013) PINK1 is degraded through the N-end rule pathway. *Autophagy* **9**, 1758–1769. doi:10.4161/auto.24633.

Yang E. S. and Park J. W. (2011) Knockdown of cytosolic NADP(+) -dependent isocitrate dehydrogenase enhances MPP(+) -induced oxidative injury in PC12 cells. *BMB Rep.* **44**, 312–316. doi:10.5483/BMBRep.2011.44.5.312

Yao Z., Gandhi S., Burchell V. S., Plun-Favreau H., Wood N. W. and Abramov A. Y. (2012) Cell metabolism affects selective vulnerability in PINK1-associated Parkinson's disease. *J. Cell Sci.*. doi:10.1242/jcs.088260.

Yuan X. L., Guo J. F., Shi Z. H., Xiao Z. Q., Yan X. X., Zhao B. L. and Tang B. S. (2010) R492X mutation in PTEN-induced putative kinase 1 induced cellular mitochondrial dysfunction and oxidative stress. *Brain Res.* **1351**, 229–237. doi:10.1016/j.brainres.2010.06.005.

Zhou T. B. and Qin Y. H. (2013) Signaling pathways of prohibitin and its role in diseases. *J. Recept. Signal Transduct. Res.* **33**, 28–36. doi:10.3109/10799893.2012.752006.

Zhou Z. D., Refai F. S., Xie S. P., Ng S. H., Chan C. H., Ho P. G., Zhang X. D., Lim T. M. and Tan E. K. (2014) Mutant PINK1 upregulates tyrosine hydroxylase and dopamine levels, leading to vulnerability of dopaminergic neurons. *Free Radic. Biol. Med.* **68**, 220–233. doi:10.1016/j.freeradbiomed.2013.12.015.

Zhu J. H., Kulich S. M., Oury T. D. and Chu C. T. (2002) Cytoplasmic aggregates of phosphorylated extracellular signal-regulated protein kinases in Lewy body diseases. *Am. J. Pathol.* **161**, 2087–2098. doi:10.1016/S0002-9440(10)64487-2.

Zhu J. H., Guo F., Shelburne J., Watkins S. and Chu C. T. (2003) Localization of phosphorylated ERK/MAP kinases to mitochondria and autophagosomes in Lewy body diseases. *Brain Pathol.* **13**, 473–481.